Modulation of Cyclobutane Pyrimidine Dimer Formation in a Positioned Nucleosome Containing Poly(dA·dT) Tracts†

Uwe Schieferstein and Fritz Thoma*

Institut für Zellbiologie, ETH-Hönggerberg, CH-8093 Zürich, Switzerland

Received December 20, 1995; Revised Manuscript Received April 5, 1996⊗

ABSTRACT: We have used a defined-sequence nucleosome to concomitantly investigate the generation and location of DNA lesions in nucleosomes and their influence on nucleosome positioning (translational and rotational setting). A 134 bp HISAT sequence from the yeast DED1 promoter, containing a polypyrimidine region (40 bp) with a T_6-tract, two T_5-tracts, and a T_9-tract, was reconstituted in nucleosomes with a defined rotational setting. T-tracts adopt unusually rigid DNA structures in solution ("T-tract structure") and are hot spots of cyclobutane pyrimidine dimer (CPD) formation by UV light (254 nm). DNA was irradiated with UV light before or after reconstitution. The CPD yields and distribution were analyzed by cleavage with T4 endonuclease V. The rotational setting of nucleosomal DNA was characterized by DNase I digestion. With the exception of one T_5-tract ($^1T_5$), the T_6-, the $^2T_5$-, and the T_9-tracts formed T-tract structure in solution. T-tract structure was lost upon folding in nucleosomes, demonstrating a dominant constraint of DNA folding in nucleosomes over that of T-tract structure. CPD formation was strongly modulated by the nucleosome structure, but the CPD distribution differed from that reported for mixed-sequence DNA. CPD formation in the nucleosome had no effect on the rotational setting of nucleosomal DNA, but the rotational setting was affected when nucleosomes were assembled on damaged DNA. The toleration of DNA distortions imposed by CPDs in nucleosomes may have important implications for the recognition and repair of these damages in chromatin.

Cyclobutane pyrimidine dimers (CPDs)[1] and pyrimidine (6−4) pyrimidone photoproducts [(6−4)PDs] are the two major stable photoproducts in UV-irradiated DNA. Their yield is dependent on the sequence [Haseltine et al., 1980; Lippke et al., 1981; for a review see Sage, (1993)], the methylation status of cytosines (Brash & Haseltine, 1982; Pfeifer et al., 1991), the DNA structure (Lyamichev et al., 1990; Lyamichev, 1991; Tang et al., 1991), and the binding of sequence-specific proteins to DNA (Becker & Wang, 1984; Wang & Becker, 1988; Pfeifer et al., 1991, 1992; Tornaletti & Pfeifer, 1995). In order for dimerization to occur, adjacent pyrimidine bases must rotate substantially from their average B-form DNA conformation. Analyzing the electrophoretic mobility of multimers of oligonucleotides containing site-specific thymine−thymine dimers, Wang and Taylor (1991) determined the thymine dimer to bend DNA by about 7°. This is in agreement with the observation of a 9° bending in the DNA helix of a decamer containing a single thymine dimer as determined by nuclear magnetic resonance (NMR) spectroscopy (Kim et al., 1995). Replacement of the site-specific CPD by a thymine−thymine (6−4)PD led to 44° helical bending (Kim & Choi, 1995).

In eukaryotic cells, the DNA is folded in nucleosomes, chromatin fibers, and higher order chromatin structures. Before we can understand how DNA lesions are repaired in eukaryotic cells, we need to know how lesions are formed in chromatin and whether and how they affect chromatin structure. Some general principles are applicable: (i) Distortions of DNA structure introduced by folding into chromatin may affect damage formation. (ii) DNA structure may be fixed by protein−DNA interactions and, hence, prevent the conformational changes that are required for damage formation. (iii) Accessibility of DNA and, hence, DNA lesions is restricted on the chromatin surface by steric exclusion and, consequently, affects DNA-damage formation by bulky reagents or damage recognition by proteins. (iv) Dynamic properties of chromatin, such as dissociation/reassociation, nucleosome mobility, folding, and unfolding will affect DNA distortions and accessibility.

This paper focuses on mutual effects of UV-induced damage formation and nucleosome core structure. The nucleosome core consists of 145 base pairs (bp) of DNA wrapped in 1.8 left-handed superhelical turns around a histone octamer. The DNA has an inner surface that faces the histones and an outer surface that faces the solution. The inner and outer surfaces define the orientation of nucleosomal DNA ("rotational setting"). The B-form DNA double helix is substantially distorted. It exhibits several regions of tight bending (Richmond et al., 1984), and the three central turns of nucleosomal DNA are underwound (10.7 bp per turn), whereas the flanking regions are overwound (10.0 bp per turn) compared to the average helical periodicity (10.5 bp per turn) of DNA in solution (Hayes et al., 1990).

When photoproducts were analyzed in nucleosome cores isolated from UV-irradiated chromatin, (6−4)PDs were almost randomly distributed (Gale & Smerdon, 1990). In contrast, CPD maxima were observed with a 10.3 bp average

† This study was supported by grants of the Swiss National Science Foundation and the ETH Zürich (to F.T.). U.S. is a recipient of a predoctoral scholarship of the Studienstiftung des deutschen Volkes (Bonn).

* Corresponding author [(41)-1-633-3323 (phone), (41)-1-633-1069 (FAX), thoma@cell.biol.ethz.ch (e-mail)].

⊗ Abstract published in *Advance ACS Abstracts,* May 15, 1996.

[1] Abbreviations: bp, base pair; CPD, *cis-syn* cyclobutane pyrimidine dimer; (6−4)PD, pyrimidine (6−4) pyrimidone photoproduct; UV, ultraviolet; T4 endo V, T4 endonuclease V; MU, map unit; DMSO, dimethyl sulfoxide.

S0006-2960(95)03011-X CCC: $12.00

periodicity very similar to the cutting pattern obtained by DNase I (Gale et al., 1987; Gale & Smerdon, 1988; Pehrson, 1989, 1995). The same modulation of CPD formation was observed in UV-irradiated isolated nucleosome cores (Gale et al., 1987) which is consistent with a preferential formation of CPDs at sites where the DNA minor groove faces the solution. A similar periodic CPD pattern generated in a DNA loop (Pehrson & Cohen, 1992) and a loss of the periodicity observed in unfolded nucleosomes (Brown et al., 1993) showed that DNA curvature is a major parameter for the modulation of CPD formation in nucleosomes. When polynucleosomes were reconstituted on irradiated calf thymus DNA, and nucleosome cores were isolated, the CPD distribution was similar to that of irradiated nucleosomes, demonstrating that CPDs were preferentially accommodated during nucleosome assembly on mixed-sequence DNA (Suquet & Smerdon, 1993).

Nucleosomes are dynamic structures. They may dissociate and reassemble, and unfold, and the histone octamer may slide along the DNA (nucleosome mobility) (Meersseman et al., 1992) in vitro and in vivo [for a review see Van Holde (1989)]. Several states may exist in a dynamic equilibrium. Known parameters that affect nucleosome positioning are DNA-sequence, flanking chromatin structures and chromatin folding [for a review see Thoma, (1992)]. The mixed-sequence experiments described above did not clarify to what extent the lesions were formed at those sites or whether they were moved into those positions by changing nucleosome positions and the rotational setting of DNA after UV irradiation. The results obtained by irradiation of isolated nucleosome cores (Gale et al., 1987) did not exclude an effect of CPDs on the rotational setting.

In contrast to mixed-sequence nucleosomes which do not allow a direct correlation between the rotational setting of DNA and damage accommodation on the nucleosome surface, we used the advantage of reconstitution of a nucleosome positioned on a defined sequence (HISAT) containing a polypyrimidine region with several T-tracts (Losa et al., 1990). This enabled us to concomitantly analyze CPD formation over three helical turns in the nucleosome and its effect on the rotational setting. The results show a complex interdependence of sequence-dependent DNA structure, nucleosome structure, and CPD formation in a positioned nucleosome.

MATERIALS AND METHODS

Preparation of Nucleosome Core Particles. Nucleosome core particles depleted of histones H1 and H5 were prepared from chicken erythrocyte nuclei as described (Lutter, 1978; Bates et al., 1981) except that the linker histones were removed by sucrose-gradient centrifugation in 650 mM NaCl, 10 mM Tris-HCl, pH 8.0, and 0.2 mM EDTA. The concentrations of DNA and protein of the core particles were quantified spectrophotometrically ($1A_{260nm} = 50$ ng/μL) and by a protein assay (Bio-Rad), respectively. Core particles (2.1 mg/mL) were stored in 10 mM Tris-HCl (pH 7.6), 1 mM EDTA, and 10 mM NaCl at −70 °C.

Preparation of End-Labeled DNA. The plasmid p9HISAT (Losa et al., 1990) was cut with *Eco*RI, and the ends were filled in with dATP and [α-^{32}P]dTTP (Amersham) using Klenow enzyme (Boehringer). After a second cleavage with *Acc*I, the uniquely labeled HISAT fragment was gel purified (Maxam & Gilbert, 1980).

Nucleosome Reconstitution. Reconstitution was by histone octamer transfer as described (Losa et al., 1990). End-labeled DNA (2×10^6 cpm; about 50 ng) was mixed with an excess of core particles (42 μg) in the presence of 800 mM NaCl and incubated at 37 °C for 30 min. Reconstitution was accomplished by stepwise addition of TE buffer (10 mM Tris-HCl, 1 mM EDTA, pH 7.5) at room temperature over a period of 140 min with 10 min incubation times at each step. The final DNA concentration was about 125 ng of DNA/μL in 93 mM NaCl. The efficiency of the reconstitution was analyzed on agarose gels (24 cm long, 0.7% agarose in 45 mM Tris base, 45 mM boric acid, 1.25 mM EDTA, pH 8.3). Reconstituted samples were mixed with half a volume of loading buffer (0.08% xylene cyanol, 0.08% bromphenol blue, 30% glycerol) and electrophoresed for 12 h at 3.3 V/cm and 4 °C. The gel was dried onto a chromatographic paper (DE81, Whatman) and exposed to X-ray films (Fuji) at −70 °C using enhancer screens. We have noticed that the loading buffer dyes apparently destabilized the nucleoprotein complexes, resulting in a higher fraction of free DNA.

DNase I Footprinting. Reconstituted samples were adjusted to 5 mM $MgCl_2$ and incubated for 5 min at room temperature. DNase I (grade I, Boehringer) was added to a final concentration of 1.5 units/μg of DNA. Aliquots were taken after 0.5, 1.5, 3, and 6 min. Control DNA was extracted from undigested reconstituted samples and dissolved in TE (pH 7.5) and 90 mM NaCl, and 10 μg of sheared herring sperm DNA (Boehringer) was added. DNase I was added to a final concentration of 0.4 unit/μg of DNA. Aliquots were taken after 0.5 and 2 min. The reaction was stopped by adjusting the samples to 10 mM EDTA; DNA was purified by phenol/dichloromethane extraction and analyzed on denaturing 8% polyacrylamide gels (Maxam & Gilbert, 1980).

UV Irradiation. Naked DNA was irradiated in TE (pH 7.5) with or without 50% (v/v) DMSO at concentrations less than 10 ng/μL. Reconstituted samples were irradiated in TE (pH 7.5) and 93 mM NaCl at DNA concentrations of about 125 ng/μL. Then 20 μL droplets were pipetted on parafilm underlayed with ice and irradiated using six germicidal lamps (G15WT8, Sylvania) emitting predominantly 254 nm at a fluence of 30 W/m^2 (15 W/m^2 for UV doses less than 2 kJ/m^2). UV fluence was measured using a UVX radiometer (UVP, San Gabriel, CA).

Photoreactivation. Irradiated DNA was dissolved in 48 μL of photoreactivation buffer [50 mM Tris-HCl (pH 7.4), 50 mM NaCl, 1 mM EDTA, 10 mM dithiothreitol, 5% glycerol, 50 μg/mL bovine serum albumin (Boehringer)] and 2 μL *Escherichia coli* DNA photolyase (0.1 μg/μL, a gift of A. Sancar) was added. The solution was pipetted into an inverted Eppendorf tube cap, covered with a microscope slide to filter short-wavelength UV light, and irradiated with two fluorescent lamps (Sylvania 15 W F15T8 BLB, peak emission at 375 nm). After 60 min, fresh enzyme was added and incubation proceeded for a further 60 min.

Mapping and Quantifying of CPDs. UV-irradiated DNA was dissolved in T4 reaction buffer [20 mM Tris-HCl (pH 7.4), 10 mM EDTA (pH 8.0), 100 mM NaCl, 100 μg/mL bovine serum albumin (Boehringer)] and incubated at 37 °C for 5 min. T4 endo V (100-fold diluted from a stock containing 400 ng/μL, a gift of R. S. Lloyd) was added and incubation continued for 60 min. Fresh enzyme was added after 15, 30, and 45 min to ensure complete digestion.

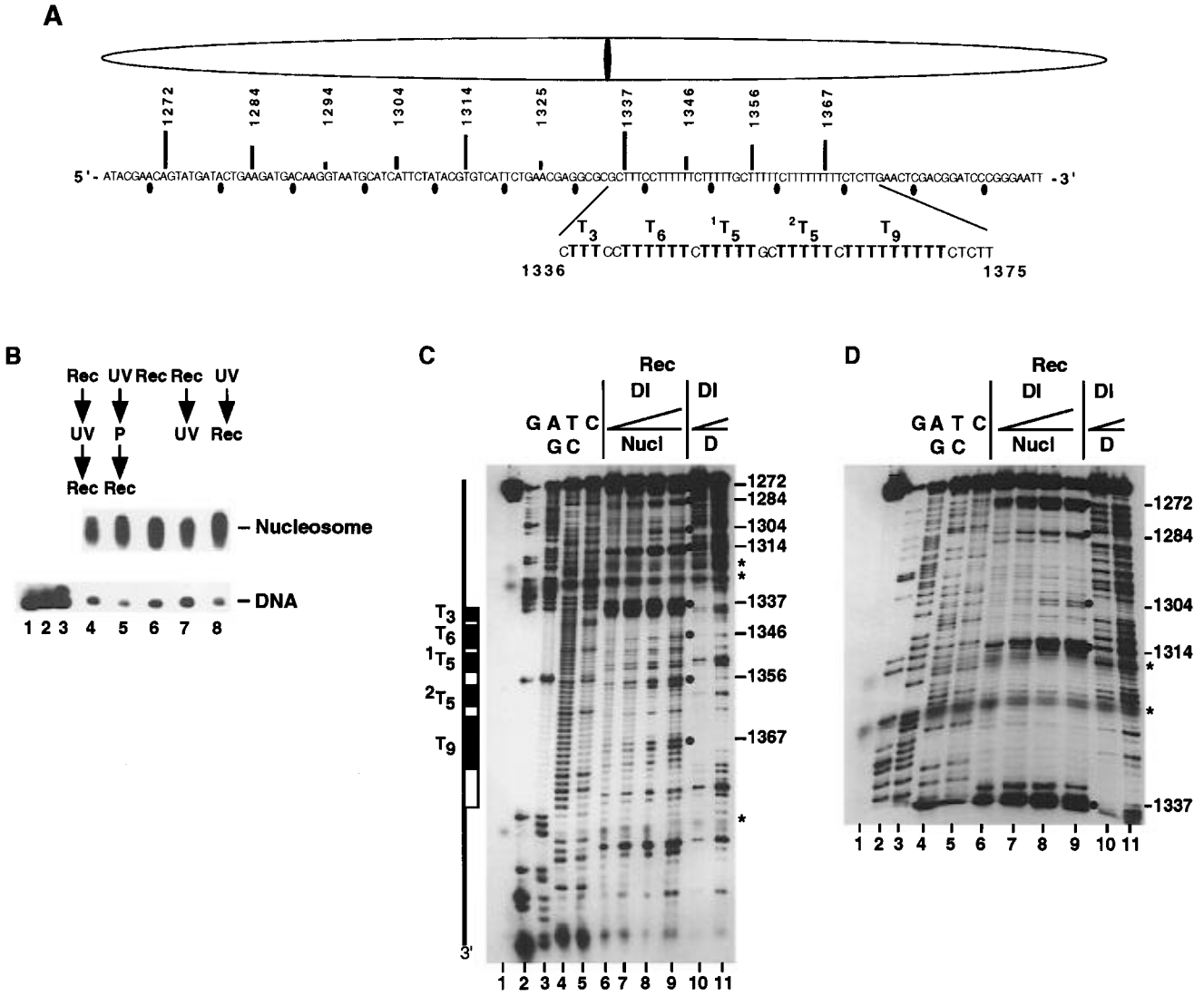

FIGURE 1: HISAT nucleosome. Panel A: The sequence of HISAT (top strand) with the polypyrimidine region containing the T-tracts (T_3, T_6, $^1T_5$, $^2T_5$, T_9) is shown. The numbering (in map units, MU) is according to Losa et al. (1990). Prominent DNase I cutting sites on the HISAT nucleosome are shown as bars above the sequence with their relative intensities indicated by the length of the bars. DNase I cutting at MU 1272 means cutting between MU 1272 and 1273. The putative location of the histone octamer on the sequence and the position of the nucleosome center are indicated (elipse). Panel B: Nucleoprotein gel of reconstituted nucleosomes. Where indicated, samples were irradiated with a UV dose of 2 kJ/m^2. Untreated DNA (lane 1); irradiated DNA (lane 2); irradiated DNA treated with photolyase (P) to remove CPDs (lane 3); untreated nucleosomes (lane 6, Rec); irradiated nucleosomes (lane 7, Rec → UV); DNA isolated from irradiated nucleosomes and reconstituted again (lane 4, Rec → UV → Rec); reconstitution with irradiated DNA (lane 8, UV → Rec) or photoreactivated DNA (lane 5, UV → P → Rec). Samples shown in lanes 6−8 were electrophoresed on a separate gel under the same conditions. The additional band above free DNA in lane 3 is an artifact due to partial denaturation of DNA. Panel C: DNase I footprint of reconstituted nucleosome cores. Nucleosomes (Nucl lanes) and protein-free DNA (D lanes) were digested by DNase I (DI) for increasing times (<). G, A/G, T/C, and C (lanes 2−5) indicate the sequencing lanes. Dots mark nucleosome-specific DNase I cutting sites; numbers show the map units. The asterisks mark an artifact due to the dyes in the loading buffer. Untreated DNA (lane 1); digestion of nucleosomes with 1.5 units/μg DNA for 0.5, 1.5, 3, and 6 min (lanes 6−9); digestion of free DNA with 0.4 unit/μg DNA for 0.5 and 2 min (lanes 10−11). The polypyrimidine region and the T-tracts are drawn to the left. (D) Long run of the gel shown in (C).

Samples for sequencing analysis were taken after 45 and 60 min. Purified digestion products were electrophoresed on denaturing 9% polyacrylamide gels (Maxam & Gilbert, 1980) until the xylene cyanol dye had run 16.5 cm. Dried gels were exposed to X-ray films (Fuji) and to a storage phosphor plate (Molecular Dynamics) and analyzed with a PhosphorImager (Molecular Dynamics) using the ImageQuant software. Volume boxes were layed around each band; background which was obtained from an equal-sized box outside of the lane was subtracted. The sum of all CPD-specific bands including the band representing the intact fragment was defined as 100%. The data presented are the means of the values obtained for the samples after T4 endo V digestion for 45 and 60 min.

Sequencing. End-labeled DNA was sequenced according to Maxam and Gilbert (1980) with minor modification. Instead of cleaving the purine residues of end-labeled DNA with piperidine formate, we used 0.5 M acetic acid and incubated samples at 45 °C for 20 min.

RESULTS

HISAT Forms a Positioned Nucleosome in Vitro. HISAT is a 134 bp long DNA sequence of the yeast DED1 promoter (Struhl, 1985). It contains an 18 and 21 bp long polypyrimidine region separated by one G and comprises five T-tracts of different lengths (Figure 1A). Using histone octamer transfer from chicken erythrocyte core particles, we have previously shown that this DNA can be folded in vitro in a

nucleosome particle with a defined rotational setting and that the T-tracts are included in the nucleosome (Losa et al., 1990). We have now used the same reconstitution protocol and UV irradiation (254 nm) at various doses before or after reconstitution to study whether and how DNA-damage formation affects nucleosome structure and vice versa. In agreement with our previous data, DNA band shift gels show that most of the labeled DNA (>90%) is incorporated in nucleosomes (Figure 1B). Both, DNase I footprinting patterns and CPD distribution patterns (see below) are consistent with high reconstitution yields.

We have deliberately chosen DNase I to probe the susceptibility of DNA on the histone octamer, since future studies are intended to address the accessibility of DNA damages on the nucleosome surface to repair proteins. DNase I digestion of the reconstituted products revealed a "10 bp ladder" extending from map unit (MU) 1272 to 1367 (Figure 1C,D, dots), demonstrating that the polypyrimidine region (MU 1336−1375) was wrapped around the histone octamers. Frequent cutting by DNase I was observed at MU 1272, 1284, 1304, 1314, 1337, 1356, and 1367 (summarized in Figure 1A). The distances of these sites to the 5′ end of the top strand (MU 1264, Figure 1A) are 8, 20, 40, 50, 73, 92, and 103 bp, respectively. Sites of infrequent cutting were observed at MU 1294, 1325, and 1346 which are 30, 61, and 82 bp, respectively, away from the 5′ end. This distribution of high and low DNase I cutting sites resembles the variation of cutting frequencies observed for mixed-sequence nucleosome cores [relative high frequencies at 10, 20, 40, and 50 nucleotides from the 5′ end, low frequencies at 30, 60, and 80 nucleotides (Lutter, 1978)] and suggests that the HISAT nucleosome center is located close to MU 1336/1337 (Figure 1A) at a distance of 72−73 bp from the 5′ end of the top strand. Surprisingly, site 1337 is highly susceptible to DNase I in the HISAT nucleosome, whereas DNA is only infrequently attacked by DNase I at the dyad axis of mixed-sequence nucleosomes. The close proximity of the 5′ end of the polypyrimidine region to the nucleosome center might be responsible for this unusual characteristic of the HISAT nucleosome.

Dose−Response of CPD Formation in HISAT. For the UV experiments, we first determined the amounts of inducible damage. The top strand of HISAT−DNA was labeled at the 3′ end. DNA or nucleosomes were irradiated with UV light (254 nm) at doses between 0.24 and 4 kJ/m^2. Purified DNA was cut with T4 endo V at CPDs. Digestion products were run on sequencing gels and quantified by PhosphorImager analysis (e.g., in Figures 3 and 4). Overall CPD yields increased with increasing UV doses and reached a plateau at doses above 2 kJ/m^2 (Figure 2) due to the reversibility of CPD formation (Haseltine et al., 1980). No obvious difference in the overall CPD yields was observed between nucleosomes and naked DNA. Assuming a Poisson distribution of the damaged fragments (Bohr & Okumoto, 1988), the average yields were 0.4, 1.2, 2.4, and 2.8 CPDs at UV doses of 0.24, 1, 2, and 4 kJ/m^2, respectively.

DNA Structure of T-Tracts in HISAT. Irradiation of naked DNA induced CPDs at every dipyrimidine sequence (Figure 3, lanes 4, 8, and 9). Runs of intensive bands corresponding to thymine−thymine (TT) dimer sites were separated by much weaker bands which located at sites containing a C (CT, TC, CC). The observed sequence dependence of CPD

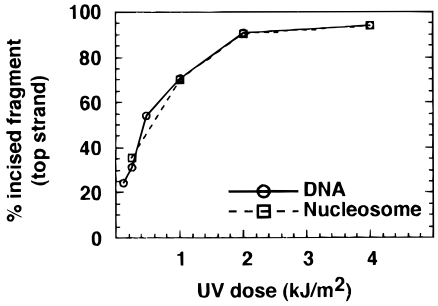

FIGURE 2: Dose−Response of CPD formation in HISAT. DNA or nucleosomes were irradiated with increasing UV doses. At 120 and 480 J/m^2, data are shown for DNA only. Purified DNA was digested with T4 endo V, run on sequencing gels and quantified by PhosphorImager analysis. The amount of the top strand incised by T4 endo V was plotted against the UV dose. Total CPD formation in the top strand was similar in nucleosomes and DNA.

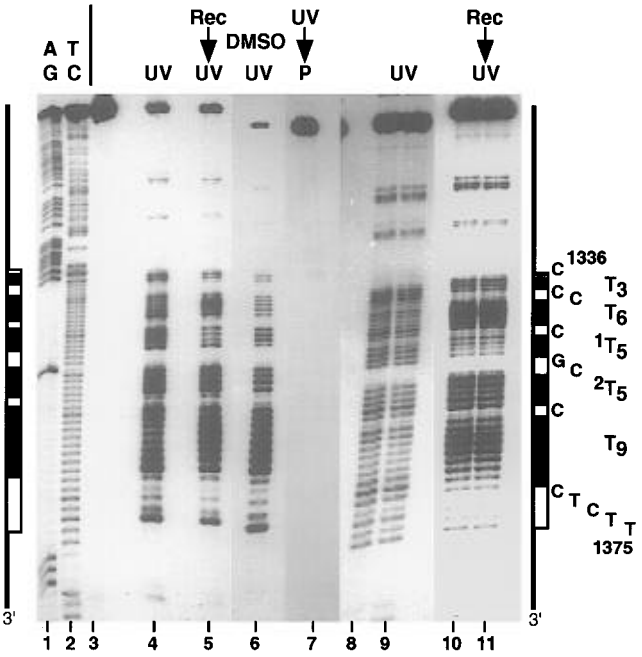

FIGURE 3: Nucleosome structure and DMSO differently modulate CPD formation in HISAT. DNA or nucleosomes were irradiated with 0.24 or 2 kJ/m^2. Purified DNA was digested with T4 endo V and analyzed on sequencing gels. A/G and T/C (lanes 1−2) are sequencing lanes. Digestion of untreated DNA with T4 endo V (lane 3) demonstrates the absence of any unspecific nicking activity. DNA irradiated with 2 kJ/m^2 (lane 4, UV) or 0.24 kJ/m^2 (lanes 8−9; sample was digested for 45 and 60 min, respectively); nucleosomes irradiated with 2 kJ/m^2 (lane 5, Rec → UV) or 0.24 kJ/m^2 (lanes 10−11; sample was digested for 45 and 60 min, respectively); DNA irradiated with 2 kJ/m^2 in 50% DMSO (lane 6, DMSO); irradiated DNA (2 kJ/m^2) treated with photolyase (lane 7, UV → P). The polypyrimidine region (MU 1336−1375, open rectangle) and the T-tracts (black bars) are indicated. The locations of the T-tracts are orientated relative to the CPDs formed in the T-tracts which are shifted relative to the sequencing markers. The T4 endo V cleaved DNA migrates one base slower than the Maxam−Gilbert sequencing product of the 5′ pyrimidine of the corresponding dipyrimidine sequence (compare lanes 2 and 4).

formation was consistent with previous results (Haseltine et al., 1980; Brash & Haseltine, 1982). Quantitation of damage formation in naked DNA is shown in Figure 4 (black bars). Signal intensities were higher toward the 3′ end label at higher UV doses (>0.5 kJ/m^2) at which more than a single CPD per molecule was induced, but the overall CPD pattern with respect to the nearest neighbors was similar for all UV doses.

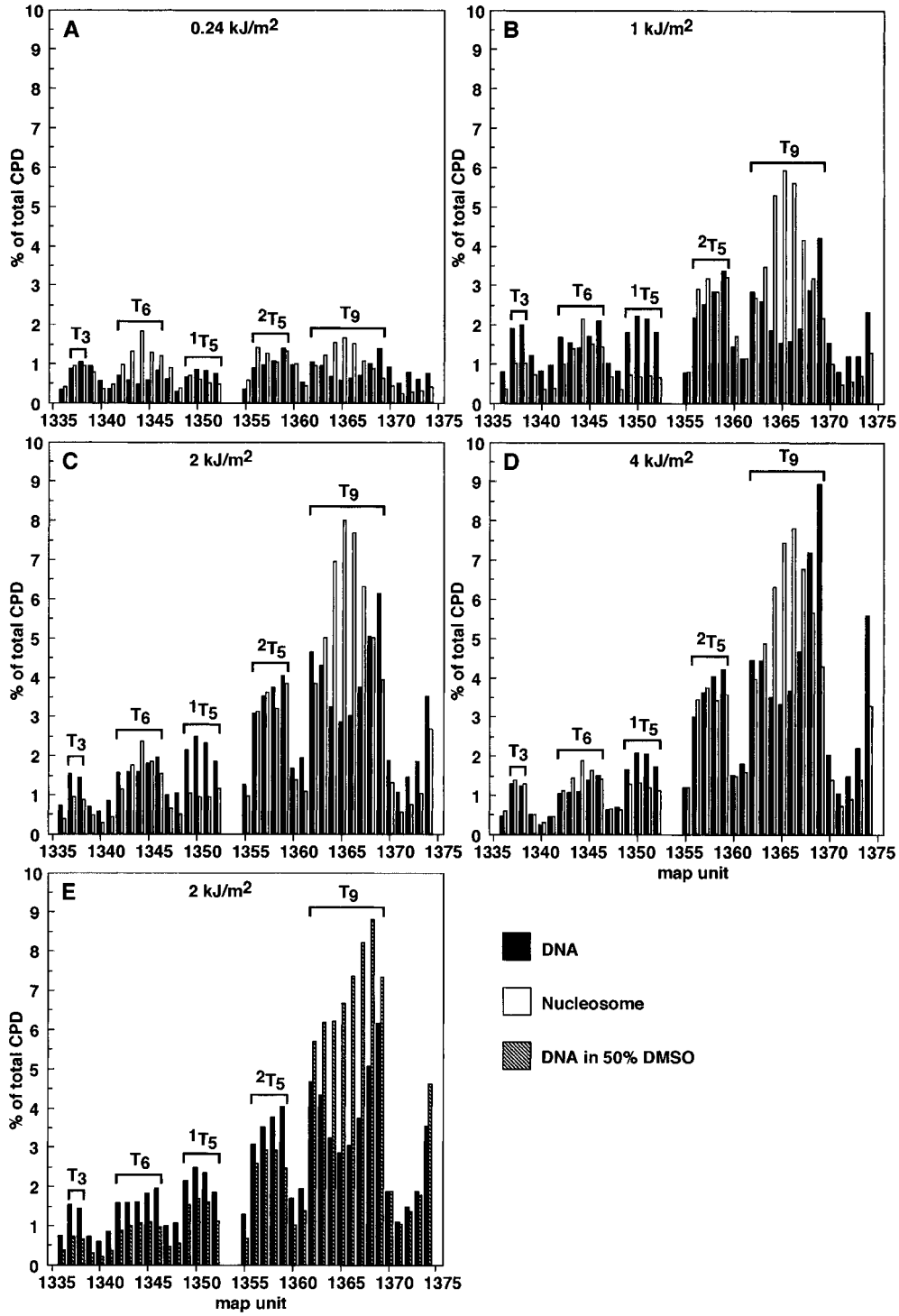

FIGURE 4: Dose−response of CPD formation in free DNA versus nucleosomes. The HISAT fragment was irradiated with different UV doses (254 nm) either before or after reconstitution. CPD formation was quantified as described in Materials and Methods. The graphs show the percentage of the total CPD yield at every individual dipyrimidine sequence within the polypyrimidine region. The map unit is given for the 5′ pyrimidine of a CPD. Black bars indicate CPD yields in DNA; open bars indicate CPD yields in nucleosomes. Panel A: 0.24 kJ/m^2. Panel B: 1 kJ/m^2. Panel C: 2 kJ/m^2. Panel D: 4 kJ/m^2. Panel E: DMSO alters photoreactivity in HISAT−DNA differently than in nucleosome structure. DNA was irradiated with 2 kJ/m^2 in 50% DMSO and analyzed as described above (stippled bars). Data for DNA irradiated in TE buffer are taken from panel C. The CPD yields in the T_3-, the T_6-, and the T_5-tracts are reduced due to the higher total CPD yield in HISAT in DMSO.

Imino proton NMR studies of T-tracts in solution revealed that the T-A base pairs, except for the 3′-terminal one, exhibited anomalously long lifetimes as compared to B-DNA sequences (Leroy et al., 1988), indicating that the structure is rather rigid. The lifetime of the 5′-terminal T-A base pair was affected by the flanking nucleotide (Leroy et al., 1988). These observations correlate well with the photoreactivity of T-tracts in which CPD yields were maximal at the 3′-terminal TT site and low at all other TT sites, and photoreactivity increased at the 5′ end when the T-tract was separated by a single C on its 5′ side from another T-tract (Lyamichev, 1991). In the T_9-tract, which is separated by a single C from the 5′-flanking T-tract, yields were minimal in the middle of the tract and increased toward both ends with the maximum at the 3′ end (Figure 4A−D). At 0.24 and 1 kJ/m^2, a similar pattern was observed in the T_6-tract

which is flanked by two C's on its 5′ side (Figure 4A,B). At 2 and 4 kJ/m^2, the TT dimer at the 5′ end was not enhanced (Figure 4C,D). Photoreactivity in the $^2T_5$-tract decreased gradually from the 3′ end to the 5′ end. The CPD patterns in the T_9-, the T_6-, and the $^2T_5$-tracts are taken as evidence for "T-tract structure" in solution (Lyamichev, 1991). The T_3-tract exhibited similar photoreactivity at both possible dimer sites. Surprisingly, the photoreactivity of the $^1T_5$-tract was high in the middle of the tract and slightly lower at both ends (Figure 4A−D), which suggests that the structure of the $^1T_5$-tract differs from that of the other T-tracts.

Dimethyl sulfoxide (DMSO) unwinds DNA by dehydration (Lee et al., 1981), perturbs the unusual T-tract structure with little effects on mixed sequences (Drew & Travers, 1984; Herrera & Chaires, 1989), and increases CPD yields within T-tracts (Lyamichev, 1991). Indeed, when HISAT was irradiated in 50% DMSO, CPD yields increased in the T_9-tract and the CPD patterns of both the T_6-tract and the $^2T_5$-tract were almost symmetric whereas the CPD pattern in the $^1T_5$-tract appeared to be unaffected (Figure 3, lane 6; Figure 4E, stippled bars). Hence, this further substantiates that the T_9-, the T_6-, and the $^2T_5$-tracts adopt T-tract structure in solution which is disrupted in DMSO.

Consistent with the photoreactivity of the T-tracts is their sensitivity to DNase I digestion (Figure 1C, lanes 10−11). DNase I interacts with the minor groove of DNA (Drew & Travers, 1984; Suck et al., 1988). A characteristic of T-tract structures is a narrow minor groove of the double helix (Nelson et al., 1987), which renders the DNA less susceptible to DNase I cutting (Drew & Travers, 1984; Herrera & Chaires, 1989). Within the polypyrimidine region, DNase I cuts intensively only at MU 1352 in the $^1T_5$-tract whereas the other T-tracts were resistant to DNase I digestion. This differential susceptibility to DNase I is presumably related to a difference in the minor groove width of the T-tracts. In summary, the results on irradiation and DNase I digestion of HISAT−DNA showed that the T_9-, the T_6-, and the $^2T_5$-tracts adopt characteristic T-tract structures in solution. However, we have no evidence for a T-tract structure in the $^1T_5$-tract.

Nucleosome Structure Modulates T-Tract Structure and CPD Formation. HISAT−DNA was reconstituted into nucleosomes and irradiated with 0.24−4 kJ/m^2, DNA was extracted, and CPDs were mapped as described for irradiated naked DNA. Results are shown in Figure 3 (lanes 5, 10, and 11) and Figure 4A−D, open bars). CPD formation in nucleosomes was drastically altered compared to irradiated naked DNA. The effects did not depend on the UV dose. Most obvious were the effects on the T_9- and the T_6-tracts, which both showed maximal CPD yields in the center and reduced yields at the 3′ end and the 5′ end. CPD formation at the 3′-terminal TT site of the T_9-tract (MU 1369−1370) was maximal in naked DNA yet low in nucleosomes. Compared with naked DNA, CPD yields were significantly reduced in the $^1T_5$-tract and also at the 3′ end of the polypyrimidine region (MU 1369−1375). Photoreactivity in the $^1T_5$-tract was always lower than in the $^2T_5$- and the T_6-tracts. In the $^2T_5$-tract, the CPD yields were similar throughout the tract (MU 1356−1360) but higher and lower at the 5′ end and the 3′ end, respectively, when compared with naked DNA (black bars). These results demonstrate that folding of DNA in nucleosomes strongly modulates CPD damage formation which apparently reflects the local distortion of nucleosomal DNA. Furthermore, the results show that T-tract structure is lost when folded in a nucleosome.

Reconstitution with Irradiated DNA Changes the Rotational Setting. DNA distortions introduced by CPDs could affect the rotational setting of nucleosomal DNA to optimize accommodation of DNA lesions. HISAT−DNA was irradiated and reconstituted into nucleosomes, and the rotational setting was analyzed by DNase I digestion. Figure 5 shows the results obtained for irradiation with 2 kJ/m^2. Nucleoprotein analysis of reconstitution products showed that UV irradiation did not dramatically affect the efficiency of nucleosome reconstitution (Figure 1B, lanes 6 and 8). The CPD pattern of DNA used for reconstitution is shown (Figure 5A, lane 8). The DNase I pattern of naked DNA was unaffected by CPDs (compare Figure 5A, lanes 14−15, and Figure 1C, lanes 10−11). This is expected, since the fraction of molecules containing a lesion at a defined MU is below 7% (Figure 4C). However, the DNase I footprints of nucleosomes reconstituted with damaged or undamaged DNA were clearly different (compare Figure 5A,B, lanes 10−13, and Figure 1C,D, lanes 6−9; see Figure 7A,B, lanes 1 and 2). In particular, cutting in the polypyrimidine region at MU 1356/57 and MU 1367/68 was not enhanced, and nucleosomal DNA between MU 1272 and MU 1314 was less well protected against DNase I. Similar results were obtained at UV doses of 1 and 4 kJ/m^2. At 0.24 kJ/m^2, the CPD yields were too small to detect an effect on reconstitution (not shown). These results strongly suggest that the population of reconstituted nucleosomes exhibited altered rotational settings of the irradiated DNA on the nucleosome surface.

In order to test whether CPDs were responsible for the observed effects, irradiated DNA was treated with photolyase, which removed the CPDs (Figure 5A,B, lane 9). This DNA containing only (6−4)PDs was used for reconstitution. Reconstitution efficiency (Figure 1B, lane 5) and the DNase I pattern (Figure 5A,B, lanes 16−19) were very similar to that obtained for undamaged nucleosomes (Figures 7A,B, lanes 1 and 3). In particular, cutting was observed in the polypyrimidine region at MU 1356/57 and MU 1367/68, and clear protection was observed between the specific cutting sites in the region from MU 1272 to MU 1314. This result demonstrates that indeed CPDs and not the low amount of (6−4)PDs produced the altered population during reconstitution. This experiment, however, does not generally exclude an effect of (6−4)PD on nucleosome reconstitution. Addressing this question would require DNA fragments enriched in TC sequences which produce higher yields of (6−4)PDs upon UV irradiation.

Formation of CPDs in HISAT Nucleosomes Does Not Change the Rotational Setting. Since CPDs and folding of DNA in nucleosomes distort DNA structure, CPD formation in nucleosomes might alter the rotational setting to optimize damage accommodation. This hypothesis was tested by comparison of the DNase I patterns of nucleosomes before and after UV irradiation. The DNase I digestion of reconstituted HISAT nucleosomes irradiated with 2 kJ/m^2 is shown in Figure 6A,B (lanes 10−13). No striking differences were observed between the DNase I patterns of irradiated and nonirradiated nucleosomes (Figure 7A,B, lanes 1 and 4), which shows that formation of CPDs in nucleosomes did not change the rotational setting. Increasing temperature was shown to facilitate histone octamer mobility

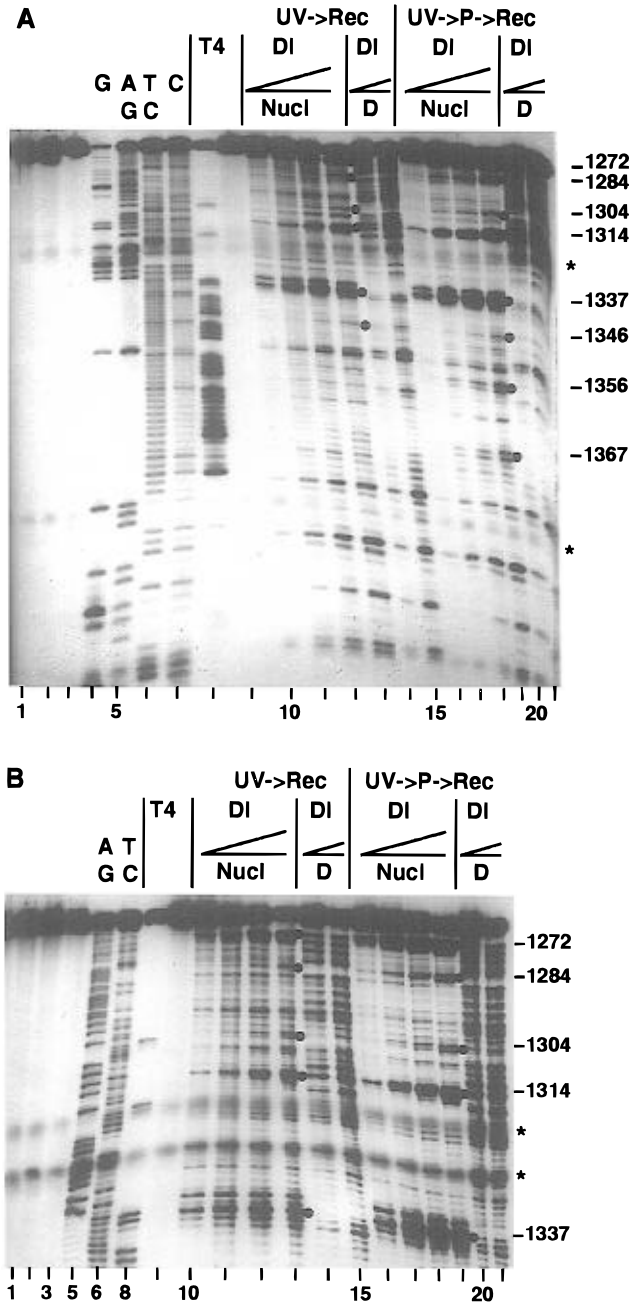

FIGURE 5: Panel A: CPDs change the rotational setting of nucleosomes during de novo assembly. The HISAT fragment was irradiated (254 nm) with a UV dose of 2 kJ/m^2 (lane 8). A fraction of the irradiated DNA was treated with photolyase in order to remove the CPDs (lane 9). Irradiated and photoreactivated DNA were reconstituted into nucleosomes (UV → Rec and UV → P → Rec, respectively) and digested with DNase I (Nucl lanes). DNA from undigested nucleosomes was purified and digested with DNase I for comparison (D lanes). G, A/G, T/C, and C (lanes 4−7) indicate the sequencing lanes. Dots mark nucleosome-specific DNase I cutting sites; numbers show the map units. The asterisks mark an artifact due to the dyes in the loading buffer. No unspecific bands were observed in irradiated free DNA (lane 1), untreated DNA digested with T4 endonuclease V (lane 2), or photoreactivated DNA (lane 3), demonstrating that neither of these treatments affected DNA. Nucleosomes reconstituted with irradiated DNA (lanes 10−13) and free DNA control (lanes 14−15); nucleosomes reconstituted with photoreactivated DNA (lanes 16−19) and free DNA control (lanes 20−21). Panel B: Long run of the gel shown in panel A.

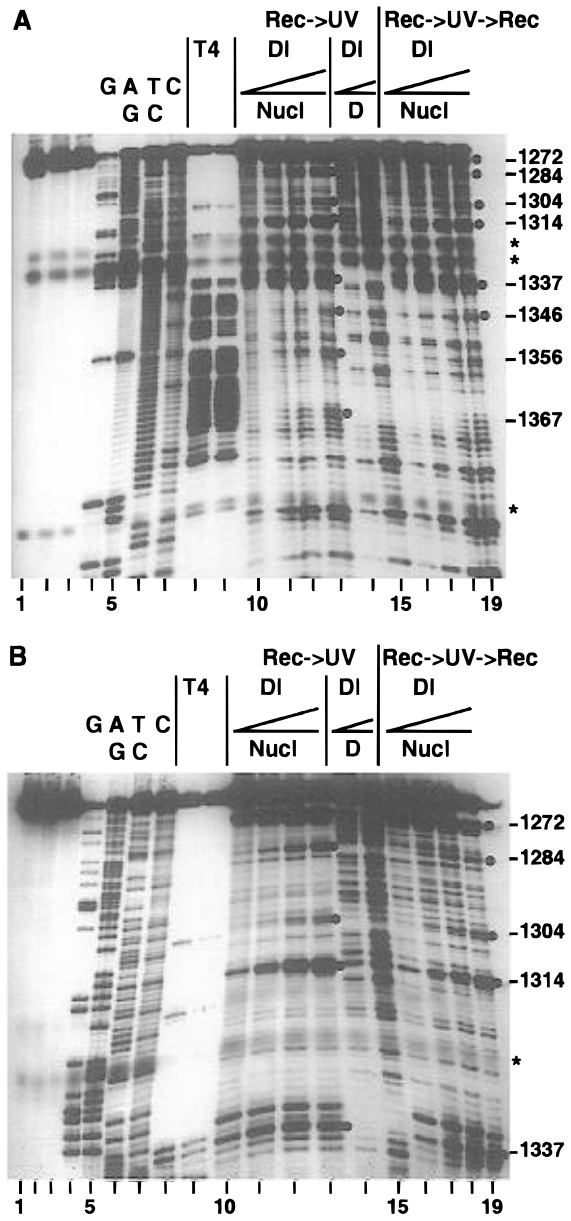

FIGURE 6: Panel A: Formation of UV damages in nucleosomes does not change the rotational setting. Reconstituted nucleosomes were irradiated (254 nm) with a UV dose of 2 kJ/m^2 and analyzed by DNase I digestion (Rec → UV). DNA purified from undigested irradiated nucleosomes was used for CPD mapping (T4 lanes) or digested with DNase I (D lanes) or reconstituted again into nucleosomes and digested with DNase I (Rec → UV → Rec). G, A/G, T/C, and C (lanes 4−7) indicate the sequencing lanes. Dots mark nucleosome-specific DNase I cutting sites; numbers show the map units. The asterisks mark an artifact due to the dyes in the loading buffer. Untreated DNA (lane 1); irradiated DNA (lane 2); untreated DNA digested with T4 endo V (lane 3). For comparison, CPDs were mapped in irradiated free or nucleosomal DNA (lanes 8 and 9, respectively). Irradiated nucleosomes (lanes 10−13); free DNA purified from undigested irradiated nucleosomes (lanes 14−15); nucleosomes reconstituted with irradiated nucleosomal DNA (lanes 16−19). Panel B: Long run of the gel shown in panel A.

on 5S rDNA but maintaining the rotational setting (Pennings et al., 1991; Meersseman et al., 1992). Incubation of the irradiated nucleosomes at 37 °C for 60 min had no effect on this particular nucleosome (not shown), although this DNA can generate different rotational settings during reconstitution (see below).

Given the results described above, CPDs formed in nucleosomes are either perfectly accommodated or the histone−DNA interactions maintaining the rotational setting are stronger than the constraints imposed by imperfect accommodation of CPDs. In order to test this hypothesis, nucleosomes were irradiated to form a nucleosome-specific

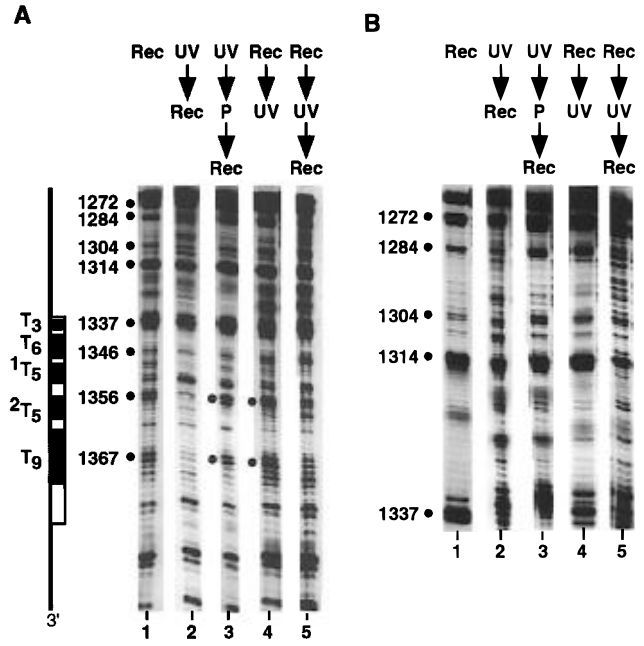

FIGURE 7: Comaparative summary of DNase I digestions. Short runs are shown in panel A: lane 1 is from Figure 1C, lane 9; lane 2 is from Figure 5A, lane 13; lane 3 is from Figure 5A, lane 19; lane 4 is from Figure 6A, lane 13; lane 5 is from Figure 6A, lane 19. Cutting was strong at MU 1356 and 1367 in lanes 1, 3, and 4 (dots) but clearly reduced in lanes 2 and 5. Long runs are shown in panel B: lane 1 is from Figure 1D, lane 9; lane 2 is from Figure 5B, lane 13; lane 3 is from Figure 5B, lane 19; lane 4 is from Figure 6B, lane 13; lane 5 is from Figure 6B, lane 19. Note the reduced protection from digestion between specific cutting sites in lanes 2 and 5.

CPD pattern, and DNA was extracted and reconstituted again (Figure 1B, lane 4). Cutting in the polypyrimidine region at MU 1356/57 and MU 1367/68 was significantly reduced (Figure 6A, lanes 16−19) compared to the DNase I pattern of irradiated nucleosomes (Figure 6A, lanes 10−13), and the DNA between MU 1272 and MU 1314 was less well protected from digestion (Figure 6B, lanes 16−19). The observed DNase I pattern strongly resembles that of nucleosomes reconstituted with DNA which was irradiated as naked DNA (Figure 7A,B, lanes 2 and 5). These results show that in a fraction of the irradiated nucleosomes DNA is constrained, but changes in the rotational setting can occur only during de novo assembly of nucleosomes.

DISCUSSION

Structure of T-Tracts in DNA and in Nucleosomes. Nucleosome core structure is characterized by tight histone−DNA contacts and substantial deformation of B-form DNA, including sharp bends and underwinding and overwinding in the center and toward the ends, respectively (Richmond et al., 1984; Hayes et al., 1990). On the other hand, T-tracts of 4 bp and longer exhibit an unusual rigid and stiff structure in solution (here referred to as T-tract structure) (Nelson et al., 1987; Leroy et al., 1988) which is therefore thought to resist formation into nucleosomes or to restrict accommodation on the nucleosome surface. However, several reports have shown incorporation of T-tracts in nucleosome cores in vitro (Losa et al., 1990; Hayes et al., 1991; Puhl et al., 1991), and statistical analysis of core particle DNA revealed that T-tracts were excluded only from the center of nucleosome cores (Satchwell et al., 1986). HISAT was previously shown to incorporate in nucleosome cores with similar efficiency as competitor DNA (Losa et al., 1990). CPD formation in T-tracts can be used to characterize T-tract structure, which shows reduced CPD yields in the central part and maximal yields at the 3′ end. The yields at the 5′ ends are increased if the flanking nucleotide is C (Lyamichev, 1991). Using this approach, we showed that the T_6-, the $^2T_5$-, and the T_9-tracts formed T-tract structure in solution.

According to our criteria the $^1T_5$-tract (5′-...CTTTTTGC...-3′) did not form T-tract structure. In contrast, imino proton NMR studies showed that a similar sequence (5′-CGCTTTTTGCG-3′) maintained properties of T-tract structure (Leroy et al., 1988). Hence, it is possible that a long-range effect related to the overall flexibility of the HISAT−DNA might destabilize the structure in the $^1T_5$-tract. On the other hand, it has been reported that dimerization at TT sites was less efficient in 5′-ATTG than in 5′-ATTA (Haseltine et al., 1980). Furthermore, several studies indicated that the base step 5′-TG possesses an unusual degree of conformational flexibility and might play a role in the formation of DNA kinks [Lyubchenko et al., 1993; for a review see Travers, (1991)]. If a localized distortion at the 5′-TG base step of the polypyrimidine region propagated through the DNA, this could compromise CPD formation at the 3′-terminal TT site of the $^1T_5$-tract and the formation of a T-tract structure. This would agree with results obtained by Becker et al. (1988), who investigated UV photoproduct formation in an *Eco*RI endonuclease−DNA complex of known crystal structure and found that an endonuclease-induced DNA kink altered photoreactivity at the adjacent base pair but failed to do so in a pyrimidine sequence 2 bp downstream.

CPD analysis of irradiated HISAT nucleosomes showed that T-tract structure was not maintained on the nucleosome surface. The altered photoreactivity in nucleosomes is not simply due to a disruption of the T-tract structure, since the CPD pattern differs from that observed for DNA in DMSO, but reflects additional deformation of DNA upon reconstitution into nucleosome cores. These results substantiate observations made by hydroxyl radical footprinting of long T-tracts (10−16 bp) incorporated in a nucleosome (Hayes et al., 1991) which showed that constraints by histone−DNA interactions dominate over T-tract structure. The strength of these interactions is underlined by our observation that the structural distortions imposed by CPD formation on nucleosomes were tolerated without changing the rotational setting. Not even incubation at higher temperature, which facilitates nucleosome mobility (Meersseman et al., 1992), was sufficient to induce a change in the rotational setting of DNA in the nucleosome population. Such a change was only achieved by disruption of the histone−DNA contacts and by de novo reconstitution.

CPD Formation in Nucleosomes. Using the HISAT defined-sequence nucleosome, we have demonstrated that CPD formation is modulated by folding of DNA in the nucleosome and that irradiation of nucleosomes did not affect the rotational setting. Hence, the CPDs found in the HISAT nucleosome reflect the distribution as it is generated during irradiation. In Figure 8, a structural interpretation is provided which summarizes the putative location of the polypyrimidine region and the CPD yields with respect to the histone surface. The path of the DNA is adopted from the low-resolution

crystal data of the nucleosome core (Richmond et al., 1984) for mixed sequences, assuming that it will not substantially deviate in the HISAT nucleosome. Based on the DNase I digestion pattern (Figure 1), the dyad is placed close to MU 1336 (arrowhead), and the major cuts for DNase I (1337, 1346, 1356, 1367) are shown where the minor grooves face outside. The CPD yields are given for an irradiation of nucleosomes with 240 J/m^2 (<1 lesion/strand) and are classified as low (white), moderate (yellow), or high (red). First of all, yields were low at sites containing a C (squares) as expected from previous work (Haseltine et al., 1980). Whether CPD formation at those sites is also modulated by the nucleosome structure cannot be answered, since there are not enough dipyrimidines containing C in this particular sequence.

Much more informative is CPD formation in the T-tracts (circles), because they spread over more than three helical turns. Several investigators studied the formation and distribution of CPDs in mixed-sequence chromatin, nucleosomes, and dinucleosomes. They all showed a modulation of CPD distribution which was consistent with relative high yields at sites where the minor grooves face outside (corresponding to preferred DNase I cutting sites) and lower yields at sites where the minor grooves face the histone octamer (Gale et al., 1987; Gale & Smerdon, 1988; Pehrson, 1989, 1995). In the HISAT nucleosome, the yields and distribution of CPDs resemble only partially those of mixed-sequence nucleosomes. For example, high yields were found close to where the minor grooves face outside (MU 1345, 1356, 1357, 1365, 1366), and low yields were found in the $^1T_5$-tract. A significant difference to the mixed-sequence data is that the CPD maxima were found 1−3 bp 5′ of the preferred DNase I cutting site. Indeed, dipyrimidines located at the DNase I site (1367) produced lower yields. In addition, HISAT was significantly different, showing high yields at sites where yields as low as in the $^1T_5$-tract were expected by extrapolation from the mixed-sequence results. This was the case, e.g., at MU 1343 in the T_6-tract and at MU 1364 in the T_9-tract.

The molecular basis for this observation is unknown. The graphic representation in Figure 8 suggests that the minor grooves at the 5′ ends of the T_6- and the T_9-tracts could be similar, while the minor groove in the $^1T_5$-tract could be more expanded. Although this representation could explain the result on HISAT, it does not explain why the corresponding sites on mixed-sequence nucleosomes do not form CPDs at enhanced rates. We therefore think that this could reflect a somewhat different accommodation of T-tracts in the nucleosome compared to mixed-sequence DNA. This difference, however, is not revealed by DNase I digestion. A more satisfying explanation has to await a high-resolution crystal structure of nucleosome cores that unambiguously will show the structure of DNA, the orientation of individual base pairs, and the histone−DNA contacts.

Our data show that the modulation of CPD formation in defined-sequence nucleosomes, as observed here, cannot unambiguously be extrapolated from the results obtained with mixed-sequence nucleosomes. They therefore illustrate the significance of investigating defined-sequence nucleosome particles in order to understand DNA-damage formation, recognition, and repair in chromatin. The HISAT sequence, which originates from the promoter region of the yeast DED1 gene (Losa et al., 1990), may appear somewhat unusual as a nucleosomal sequence. However, it is pointed out that long T-tracts are frequently found in yeast promoters (Struhl, 1985; Karlin et al., 1993) and the question whether and how they form nucleosomes in vivo (Losa et al., 1990) and how DNA damage is repaired in these regions is an important topic to be addressed.

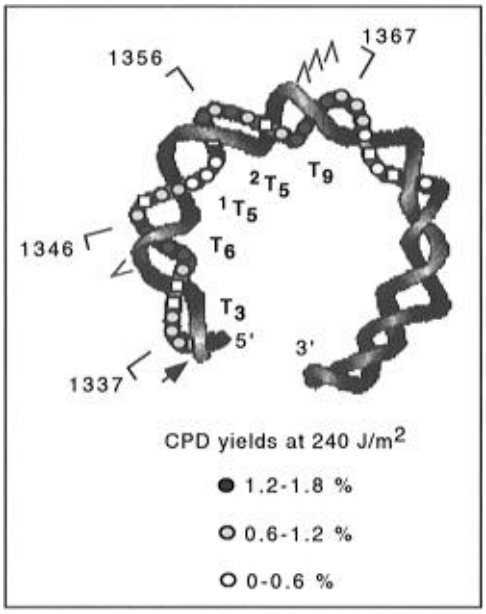

FIGURE 8: CPD formation in the HISAT nucleosome. The path of the DNA is adopted from the crystal structure of the nucleosome core (Richmond et al., 1984). The polypyrimidine region (MU 1336−1375) is indicated by circles (T base) and squares (C base). There is a gap at the position of the single G (MU 1354). CPD yields at 240 J/m^2 are classified as low (white), moderate (yellow), or high (red). Red angles represent local CPD maxima at MU 1344 and 1364−1366. Map units at the outside show DNase I cutting sites; the putative position of the nucleosome center is indicated by the arrowhead. The location of the T-tracts is shown on the inside.

ACKNOWLEDGMENT

We thank Drs. A. Sancar and R. S. Lloyd for generous gifts of *E. coli* DNA photolyase and T4 endonuclease V, Dr. C. Weissmann for the use of the PhosphorImager, and Dr. M. J. Smerdon for discussion.

REFERENCES

Bates, D. L., Butler, P. J. G., Pearson, E. C., & Thomas, J. O. (1981) *Eur. J. Biochem. 119,* 469−476.
Becker, M. M., & Wang, J. C. (1984) *Nature 309,* 682−687.
Becker, M. M., Lesser, D., Kurpiewski, M., Baranger, A., & Jen-Jacobson, L. (1988) *Proc. Natl. Acad. Sci. U.S.A. 85,* 6247−6251.
Bohr, V. A., & Okumoto, D. S. (1988) in *DNA repair: A laboratory manual of research procedures* (Friedberg, E. C., & Hanawalt, P. C., Eds.) pp 347−366, Marcel Dekker, Inc., New York.
Brash, D. E., & Haseltine, W. A. (1982) *Nature 298,* 189−192.
Brown, D. W., Libertini, L. J., Suquet, C., Small, E. W., & Smerdon, M. J. (1993) *Biochemistry 32,* 10527−10531.
Drew, H. R., & Travers, A. A. (1984) *Cell 37,* 491−502.
Gale, J. M., & Smerdon, M. J. (1988) *J. Mol. Biol. 204,* 949−958.
Gale, J. M., & Smerdon, M. J. (1990) *Photochem. Photobiol. 51,* 411−417.
Gale, J. M., Nissen, K. A., & Smerdon, M. J. (1987) *Proc. Natl. Acad. Sci. U.S.A. 88,* 6644−6648.
Haseltine, W. A., Gordon, L. K., Lindan, C. P., Grafstrom, R. H., Shaper, N. L., & Grossman, L. (1980) *Nature 285,* 634−641.
Hayes, J. J., Tullius, T. D., & Wolffe, A. P. (1990) *Proc. Natl. Acad. Sci. U.S.A. 87,* 7405−7409.

Hayes, J. J., Bashkin, J., Tullius, T. D., & Wolffe, A. P. (1991) *Biochemistry 30,* 8434−8440.
Herrera, J. E., & Chaires, J. B. (1989) *Biochemistry 28,* 1993−2000.
Karlin, S., Blaisdell, B. E., Sapolsky, R. J., Cardon, L., & Burge, C. (1993) *Nucleic Acids Res. 21,* 703−711.
Kim, J. K., & Choi, B. S. (1995) *Eur. J. Biochem. 228,* 849−854.
Kim, J. K., Patel, D., & Choi, B. S. (1995) *Photochem. Photobiol. 62,* 44−50.
Lee, C.-H., Mizusawa, H., & Kakefuda, T. (1981) *Proc. Natl. Acad. Sci. U.S.A. 78,* 2838−2842.
Leroy, J., Charretier, E., Kochoyan, M., & Gueron, M. (1988) *Biochemistry 27,* 8894−8898.
Lippke, J. A., Gordon, L. K., Brash, D. E., & Haseltine, W. A. (1981) *Proc. Natl. Acad. Sci. U.S.A. 78,* 3388−3392.
Losa, R., Omari, S., & Thoma, F. (1990) *Nucleic Acids Res. 18,* 3495−3502.
Lutter, L. C. (1978) *J. Mol. Biol. 124,* 391−420.
Lyamichev, V. (1991) *Nucleic Acids Res. 19,* 4491−4496.
Lyamichev, V. I., Frank-Kamenetskii, M. D., & Soyfer, V. N. (1990) *Nature 344,* 568−570.
Lyubchenko, Y. L., Shlyakhtenko, L. S., Appella, E., & Harrington, R. E. (1993) *Biochemistry 32,* 4121−4127.
Maxam, A. M., & Gilbert, W. (1980) *Methods Enzymol. 65,* 499−560.
Meersseman, G., Pennings, S., & Bradbury, E. M. (1992) *EMBO J. 11,* 2951−2959.
Nelson, H. C. M., Finch, J. T., Luisi, B. F., & Klug, A. (1987) *Nature 330,* 221−226.
Pehrson, J. R. (1989) *Proc. Natl. Acad. Sci. U.S.A. 86,* 9149−9153.
Pehrson, J. R. (1995) *J. Biol. Chem. 270,* 22440−22444.
Pehrson, J. R., & Cohen, L. H. (1992) *Nucleic Acids Res. 20,* 1321−1324.
Pennings, S., Meersseman, G., & Bradbury, E. M. (1991) *J. Mol. Biol. 220,* 101−110.
Pfeifer, G. P., Drouin, R., Riggs, A. D., & Holmquist, G. P. (1991) *Proc. Natl. Acad. Sci. U.S.A. 88,* 1374−1378.
Pfeifer, G. P., Drouin, R., Riggs, A. D., & Holmquist, G. P. (1992) *Mol. Cell. Biol. 12,* 1798−1804.
Puhl, H. L., Gudibande, S. R., & Behe, M. J. (1991) *J. Mol. Biol. 222,* 1149−1160.
Richmond, T. J., Finch, J. T., Rushton, B., Rhodes, D., & Klug, A. (1984) *Nature 311,* 532−537.
Sage, E. (1993) *Photochem. Photobiol. 57,* 163−174.
Satchwell, S. C., Drew, H. R., & Travers, A. A. (1986) *J. Mol. Biol. 191,* 659−675.
Struhl, K. (1985) *Proc. Natl. Acad. Sci. U.S.A. 82,* 8419−8423.
Suck, D., Lahm, A., & Oefner, C. (1988) *Nature 332,* 464−468.
Suquet, C., & Smerdon, M. J. (1993) *J. Biol. Chem. 268,* 23755−23757.
Tang, M. S., Htun, H., Cheng, Y., & Dahlberg, J. E. (1991) *Biochemistry 30,* 7021−7026.
Thoma, F. (1992) *Biochim. Biophys. Acta 1130,* 1−19.
Tornaletti, S., & Pfeifer, G. P. (1995) *J. Mol. Biol. 249,* 714−728.
Travers, A. A. (1991) *Curr. Opin. Struct. Biol. 1,* 114−122.
Van Holde, K. E. (1989) in *Chromatin*, Springer Verlag, Berlin.
Wang, C. I., & Taylor, J. S. (1991) *Proc. Natl. Acad. Sci. U.S.A. 88,* 9072−9076.
Wang, Z., & Becker, M. M. (1988) *Proc. Natl. Acad. Sci. U.S.A. 85,* 654−658.

BI953011R